Supplemental file of paper "Sensing and Decision-Making in Cyber-Physical Systems: The Case of Structural Event Monitoring"

APPENDIX A
EXTENDED COMMUNICATION NETWORK MODEL

Consider a physical structure, such as GNTVT [1], [2] for monitoring, and the WSN topology, as depicted in Fig. 3. The structure consists of a number of substructures [3], as shown in Fig. 3c, represented by Ω_q, where q is the maximum number of substructures. Suppose that we are given a set P of S homogeneous sensors with limited energy, we need to form such a WSN denoted by $W = (V, E)$ over the structure. S sensors are attached to the structure by some location assignment $L = l_1, l_2, \ldots, l_S$, where sensor s_u is placed at location l_u. We adopt an SHM-specific sensor placement model to form the WSN, according to [4] (see Appendix B), by which we can have sensor nodes like the LDM and DDM deployed. However, the link quality model of it does not show sufficient performance for WSN deployment.

We have modified the link quality model regarding dynamic structural environments (see later part of this appendix). This adopts the idea of the log-normal path loss model [5], which is a popular radio propagation model, enabling us to have the formation of IEEE 802.15.4 links into three distinct reception regions: connected, transitional, and disconnected. According to this model, the strength of a radio signal decays with some power of distance. By following the model, We let R_{min} and R_{max} denote the communication range for connected region and transitional region, respectively. We ignore the the disconnected region in our model. We take R_{min} as the range that a sensor can easily communicate with 100% packet transmission rate (PRR). In our model, any two sensor nodes within a range of R_{max} are predicted to be in communicable range of each other. We calculate R_{max} based on a statistical link quality on a initial sensor deployment. If a sensor experiences that its R_{max} (due to a long diameter of a substructure) is more than a threshold value, we attempt to deploy one/two redundant sensors around of it so that the link quality or PRR is improved.

After the deployment of all sensors, they are organized into (possibly overlapping) $g_i (i = 1, 2, \ldots, K)$ groups. Each group contains a subset of s_m sensors around a substructure for monitoring. g_i is variable, which relies on the WSN density and diameter of a substructure. We assume that the number of groups is equivalent to the number of substructures, say, $q \equiv K$. In the WSN, each sensor senses periodically to get response measurements (i.e., excitation caused by harmful vibration, heavy wind, load, etc.). Each sensor in a group works as an LDM. After the first election, one of the LDMs in the group is elected as a DDM before T_d finishes. An LDM can adjust its R_{min} according to the connected region based on diameter d, as shown in Fig. 3d. At R_{max}, a DDM can connect to its neighbor DDMs or the BS. In MODEM, new DDMs, but not new groups in the WSNs, are chosen at each T_d to provide fairness. At each T_d, a new sensor as a LDM may join or leave the group due to various environmental and fault factors, but the group still remains.

A. Wireless Link Model and Link Quality Improvement

As described in Section IVB and earlier, although we have sensor nodes like LDM and DDM deployed through a previously recently algorithms [4], such a DDM is assumed to be a high-end heterogeneous sensor node having additional energy and is set as a fixed DDM. However, we need homogenous sensors as the DDMs, and such a sensor is not a fixed DDM (any sensor has a chance to be a DDM at each data collection period in MODEM). Thus, a wireless communication link model should be more realistic than the one we adopt in [4]. Particularly, for a larger network (if planning to monitor a long-span bridge, subway tunnel, aero-space vehicle, etc.) with a large number of sensors locations, deploying fixed DDMs or relay nodes at all potential relay locations will be impractical.

What we need is a model to recognize the characteristics of the wireless channel in the structural environments so as to predict feasible links from each sensor to another sensor, and from each sensor toward the BS. While there can be many approaches for modeling the link quality, we consider an improved link quality model considering dynamic structural environments. We adopt the idea from the log-normal path loss model [5], which is a popular radio propagation model that can enable us to have the formation of IEEE 802.15.4 links into three distinct reception regions: connected, transitional, and disconnected. According to this model, the strength of a radio signal decays with some power of distance. By following the model, we let R_{min} and R_{max} denote the communication ranges for the connected region and transitional region, respectively. We ignore the disconnected region in our model. We take R_{min} as the range that a sensor can easily communicate with 100% packet transmission rate (PRR).

However, using the path loss model, it is difficult to have more than 40% PRR with R_{max}. According to the path loss model, the signal strength is also summed with random Gaussian variations. Those random variations make the PRR irregular in the transitional region that makes it difficult to analyze the wireless link behaviors. Many times, the PRR appears less than 20% if sensors are placed with high location quality according to SHM application deployment requirements [1], [4]. Thus, there are significant challenges when a sensor node needs to find R_{max}. In our model, any two sensor nodes within R_{max} are predicted to be within a communicable range of each other. We consider that R_{max} vary at different locations, at different times, and at different deployment environments (for various structures).

Link quality calculation. We calculate R_{max} through a statistical link quality estimation on the initial sensor deployment. The link quality is estimated in terms of packet

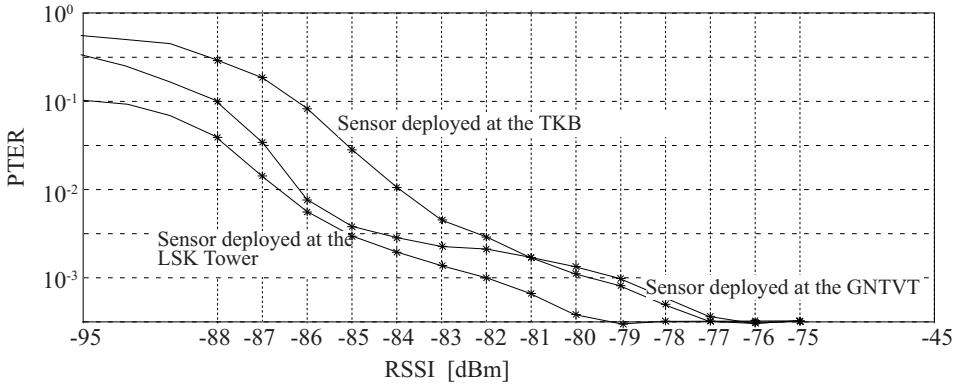

Fig. A. PTER vs. RSSI measured between two sensors for the CC2420 802.15.4 radio at three different fields, where the packet size is set to 124 bytes.

transmission error rate (PTER). The PTER comes from the bit error rate, which in turn is obtained by the sensor received signal strength, its captured noise and interference, and its modulation-demodulation scheme. During the SHM sensor deployment on the GNTVT, we have verified on-field link quality experiments with 10 Imote2 sensor platforms, particularly aiming to observe reliable R_{max} at different locations. We have also carried out similar experiments on the TKB bridge (actual name is not given do anonymity) (deploying sensors at different locations of different substructures), and the LSK building on the university campus [4]. We experimentally derive the mapping between PTER and RSSI in the case of the CC2420 802.15.4 radio, as shown Fig. A.

We configure the packet size to be 124 bytes, taking into account that it may produce high PRR under this packet size and can normally have high PRR for smaller packet sizes. We found that the PRR and PTER at any given location is random. The PTER is below 0.025 or 0.035 for RSSI values that are larger than -10 dBm, whereas below this RSSI value not only does the PTER quickly increase, but is highly variable from sensor to sensor.

From our experience gained through the link quality verification at different deployments, we find the link model in terms of R_{max}, such that with a transmitter power of 0 dBm, a receiver at range R that is less than R_{max} is very likely to receive a signal strength better than -86 dBm. The transmitter power of 0 dBm is chosen so as to minimize the requirement of DDMs. In the model, we select reliable R_{max} by utilizing existing wireless radio propagation loss models in terms of (i) the log-distance path loss model with shadowing and a stochastic fading model (which accounts for multipath fading and channel variations) [5], [6] We compute three statistical information factors as follows.

- We find the maximum PTER denoted by P_m, e.g., 0.025, that is equivalent to a minimum value of RSSI, e.g., -86 dBm.
- The PTER on a given link between any two sensors can be worse than P_m at some point, since wireless links can fade over time. At some point, the link can be faded out. The probability of a multihop path being faded out increases with the number of hops. We find a threshold **f**ading **o**ut probability, denoted by P_{fo}. The probability on a link that the link is not faded out, i.e., P'_{fo} is the fraction of packets received when the value of RSSI is a minimum value, e.g., $\geq$ -86 dBm, on the link.
- We set R as the reliable link length, by which two sensors show more than 90% reliability, $R \leq R_{max}$. f_R is a function of the link length R, and is defined as the fraction of links of length $R \leq R_{max}$ that do not have fading out threshold P_{fo}. The reason of calculating f_R is as follows: there are average path loss variations in the transitional region, from link to link due to shadowing or other related factors. f_R is compared to f'_R (which is a threshold value). When we have a reliable link by f_R, we can have an unreliable link by estimating $1 - f_R$.

Once we have all values of P_m, P_{fo}, and F_R measured from a sensor node to another, we can calculate a reliable R_{max} as follows:

R_{max}: The range R at which $f_R \geq f'_R$.

After LDM has its R_{max} to a neighboring LDM and a DDM around a substructure, the rest of the process for connecting them is described in Section IIIC. An LDM includes all the links that are of $R \leq R_{max}$. In finding this, we can analyze two factors: (i) the lower the value of f_R, the larger the possibility of reliable link on the field, and this helps to find a subset of locations with a low link reliability where a redundant sensor can be placed to improve the low link reliability to a high link reliability, as well as overall network performance.

Although existing analytical models such as Rayleigh or Ricean fading, and log-normal shadowing, can be used to calculate RSSI or P_m, P_{fo}, or f_R, the relations between them are indicative that they cannot be used for reliably characterizing the quality of links in the WSN for highly dynamic environments. We can conclude that the maximum range in which the probability of a link is good $f_R \geq f'_R$ is chosen as the maximum communication range for reliable communication.

APPENDIX B
SENSOR PLACEMENT

A very important requirement of SHM is the sensor placement by following CSMA engineering methods. One may follow the generic WSN sensor placement methods, i.e., random, uniform, or grid/tree. We assume that these may not be suitable for finding high-quality locations where the best

structural characteristic can be achieved. The sensor nodes should be placed on critical locations that are of civil/structural engineering importance. We exactly follow a civil engineering sensor deployment method, such as EFI (effective independence) model for sensor placement [7], which is most widely accepted method for SHM. In civil engineering, there is a well-accepted metric in EFI to specify the placement quality: the Fisher Information Matrix (FIM) determinant.

The main idea of EFI is as follows. When given a set of candidate locations, the location is sorted according to their contributions to the FIM determinant. Sensors are placed based on the FIM contribution. Sensor with the least contribution to the FIM quality is removed and put it together with other sensor sensors and place to some other locations where have the best contribution to FIM so as to improve best placement quality for monitoring. So a sensor is placed at a location with the best location quality. We follow a recent WSN-based SHM scheme focusing on finding the EFI determinant, high-quality location together with fault tolerance [7].

As modeled in Section IVB, we are given P of S sensors. We place a small number of redundant sensors so that we can improve the network connectivity. Let S_1 and S_2 be the number of primary and redundant sensors, respectively. Thus, we have, $m \geq S_1+S_2, S_1 > S_2$, i.e., we can separate a number of sensors as redundant sensors from the given sensors before deployment. As [7], we place S_2 sensor at points where the connectivity is poor, some sensor are isolated, or the location is not covered so that the network can have strong connection and coverage.

A structure F has a set of M feasible locations for sensor placement. *S_1 primary sensors are deployed on F by finding candidate locations out of M, using EFI values*. After deployment, S_1 sensors can be connected through clusters in a single to multi-hop WSN one time. For simplicity, we assume that the deployed WSN with S_1 primary sensors is prone to faults and is weakly connected (i.e., k-connected, $(k \geq 1)$), where sensor i is placed at l_i. It is highly possible that the network connectivity is unstable in the structural environment. It is crucial in SHM, once a set of sensors are deployed, that data must be collected from each optimal location for SHM. Thus, data delivery must be fault-tolerant in the WSN.

APPENDIX C
EXTENDED DETAIL OF THE ENERGY COST MODEL

One of the major objectives is to minimize the energy cost of the WSN. This entails making a decision on an event detection, getting a confirmation from a DDM, and getting an acknowledgment as the decision confirmation from the DDM reaches the BS. A significant amount of energy is also required in grouping and inter-grouping communications. We consider an existing energy model, suggested for clustering in a WSN-based SHM systems [8]. Regarding the model [8], we briefly describe here how energy consumed in transmitting/receiving a packet is computed in our case. Let $cost(s_u)$ be the total energy cost of a sensor in ith group g_i and $cost(g_i)$ be the energy cost of the group of sensors, which is given as follows:

$$cost(g_i) = \sum_{u=1}^{n} cost(s_u)$$

where $cost(s_u) = Er_s(s_u) + Er_c(s_u) + e_{dm}$.

We describe the terms as follows.

i) $Er_s(s_u)$ is the energy required by sensing for N data points; in taking vibration signal measurements, assuming that there is a maximum 40% overlap, $N = (n_a/2+1/2)\cdot c_r$, where n_a and c_r are the number of averages, mainly for denoising purposes. These basically vary from 10 to 20, and are cross-correlational factors [8]. n_a, c_r, and N are set by fixed values on a sensor.

ii) $Er_c(s_u)$ is the energy cost per bit for transmission over a link between a transmitter and a receiver, which includes the energy cost for sending and receiving data, and grouping and inter-grouping communication tasks. Additionally, overhead for communications is included in the energy cost calculation for data transmission.

iii) e_{dm} is given by (2). To calculate, we initially use an Imote2 how long it takes to process our decision making algorithm and the processor frequency for the algorithm. We then use the same amount of energy in the evaluation.

Note that we have tried to obtain AoED results substructure-wise (or group-wise) in MODEM. As described, the key idea behind it is to find a group-wise final decision for each substructure independently so that the existence of an event in a specific substructure can be identified by WSNs. In the energy model, we have tried to figure out the energy cost for the group that can detect an event. However, the total energy cost of a WSN definitely comes from the total energy cost of all the groups of sensors in the network, where each group consists of a number of sensors.

APPENDIX D
OVERALL PERFORMANCE OF MODEM THROUGH SIMULATIONS

In simulations in Section VIIIA, we have demonstrated that MODEM outperforms its counterparts in terms of energy cost reduction and ability of event detection (AoED). The reasons as of the performance are as follows.

A. Low Data Transmission through The Consideration of the Design of CPS.

The existing WSN schemes, DLAC, original ERA, distributed ERA, SPEM, and MODEM (centralized), which are considered in our comparison for SHM, primarily target computing system issues (like data acquisition, communication) or physical structural system issues (like damage or change event detection). However, the "network performance" of these schemes can be improved by considering the real situation in the physical process of the structural event. We provide the following discussion to support this statement.

Although wired sensors are used to determine the area of damage event location, it is difficult, if not impossible for energy and bandwidth constrained wireless nodes to continuously transmit the raw data to the designated recipient. In order to get an optimal solution, we think of two points:

TABLE I
DECISION-MAKING BY THE FIRST 15 GROUPS OF SENSORS IN EVERY FIRST ROUND OF 7 SUCCESSFUL SIMULATION RUNS OF MODEM.)

	Sensor #															
Group	1	2	3	4	5	6	7	8	9	10	11	12	13	14	15	...
Sim. 1	1	1	0	1	**1**	0	0	0	0	1	0	***1***	0	0	**1**	...
Sim. 2	1	0	0	1	**1**	0	***1***	0	1	0	0	0	0	0	0	...
Sim. 3	1	**1**	0	1	0	0	0	0	0	1	**1**	0	0	0	0	...
Sim. 4	1	0	0	0	0	0	0	0	**1**	1	0	0	0	0	**1**	...
Sim. 5	1	0	0	1	**1**	0	0	0	0	1	**1**	0	0	0	0	...
Sim. 6	1	**1**	0	1	0	0	0	0	**1**	1	0	0	0	0	0	...
Sim. 7	1	0	0	1	**1**	0	0	0	0	1	0	0	0	0	0	...

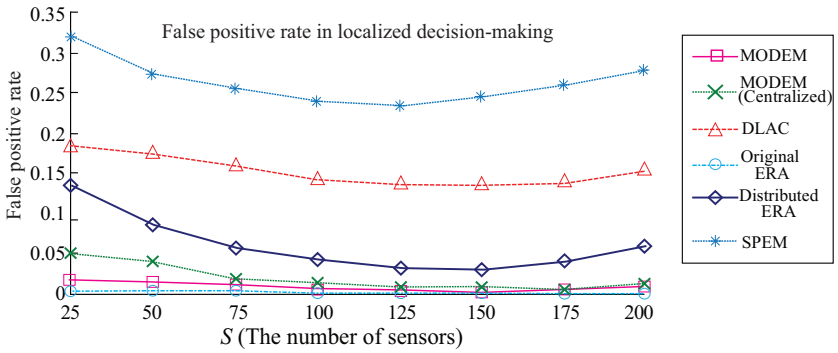

Fig. B. False positive rate in the localized decision-making in MODEM and existing schemes.

1) The situation of the event/change occurrence.
2) The specific substructure (if there is an event).

Hence, we enable the network to reduce its total energy cost by minimizing the amount of communication and computation tasks in the network based on the event occurrence in the substructure. We have provided a computation model in the CPS. Based on the model, it can be best observed that, commonly, "no change (e.g., damage)" occurs in a structure. It can also be argued that, in an unusual situation, if there is an 'event' of damage in the structure, the event may first occur in a substructure of the structure rather than occurring over the whole structure at a time. Regarding this in a resource-constrained WSN, the large volume of data really does not always need to be transmitted to the BS. Instead, a simplified decision transmission interesting in the case of a "no change" state. However, if a change has occurred in the structure, in addition to transmitting a decision on the possible change, a node may need to transmit all of its collected data towards an upstream node (cluster head) or the BS upon request. The nodes may have additional interactions between them. For example, they need to communicate to the neighboring nodes in the substructure of the change and to further analyze the data for ensuing the state of the change. This indicates that a change in the physical structural system results in extensive communication and computation in the WSN system, especially between the nodes in the substructure around the change. If there is no change/event in the structure based on our decision-making, the sensor nodes can reduce a great amount of energy cost.

B. Low False Positive Rate Leading High AoED.

There is no further use for frequent data collection and data transmission if there is no damage event. This can be achieved by the decision-making in such complex event. A precise decision, '0' for 'no damage event' situation is similar to '0/1' decision in a target detection application of WSNs. This only needs to exchange local decisions with their neighbors or the cluster head, except the case that there is an event. If there is an event, all data are required to be sent. As a result, the performance in terms of AOED is increased in MODEM compared to other schemes.

Table I depicts the results of decision-making by the first 15 groups of sensors in every first round in 7 successful simulation runs in MODEM. Some of the sensor groups in the neighboring substructures shows '1' decisions. This is because the damage event information injected into the subsets of sensors, which participate in different groups in different simulation runs, while we vary the amount of sensor group overlap from 20% to 40% when noise ratio. A boundary sensor, which has data with damage event information, may be part of the two or more groups. This sensor may provide the true positive decision (may be '1'). However, its neighboring sensors located at the neighboring substructures may also have the true positive decision (either '0' or '1'). These all decisions are the true positive decisions. However, they are some false positive decisions: '***1***' decisions (bold and italic marked in Table IV). Based on decision-making algorithm, the the false positive rate is found to be very low (zero in many simulations). However, in a case that there is a false positive decision, it is detected at the LDM level in a disturbed manner. No false positive decision is transmitted to the BS.

Fig. B shows the false positive rate in the decision-making in MODEM and other schemes. The rate in MODEM is estimated from the results, gathered from 200 simulation runs. We also come up with decision-making at a cluster head or at the BS for other schemes. This figure is evident that some

schemes such as DLAC, distributed ERA, and SPEM, show high false positive rate in the decision-making based on the reduced or whole amount of data collection at the BS. Among them, the false positive rate in SPEM and DLAC are more than 0.15. There are various reasons for having high false positive rate, including the following:

- Online decision-making in a round of monitoring under a fixed time duration T_d.
- An excessive amount of data packet losses.
- A loss of an important information during local/distributed data reduction process or compression process.
- The amount of sensor group overlapping.
- Optimal sensor placement for SHM.
- Sensor faults.

The false positive rate ($\leq$ 0.03) in decision-making in MODEM is close to the false positive rate ($\leq$ 0.02) in decision-making in original ERA scheme (which is usually required by the engineering domains).

C. Low Computation Cost

To extract structural properties and make a decision, MODEM takes lower computation cost than algorithms is those existing schemes take. The computational cost is described in Section VB.

D. Sensor Placement at High-quality Locations

Sensors are placed at high-quality locations that provide best estimate of the structural properties that make accurate decision-making. Besides, redundant sensor placed at points considering both connectivity and coverage. Thus, these lead better AoED in MODEM compared to DLAC, SPEM, original ERA, and distributed ERA.

APPENDIX E
EXTENDED SETUP DETAIL OF PROOF-OF-CONCEPT SYSTEM DEPLOYMENT ON THE PHYSICAL STRUCTURE

A. Objectives

As proof-of-concept experiments, we have implemented the MODEM in TinyOS on a SHM mote platform [9]. The objectives of this implementation are the similar to those of simulations. Particularly, we intend to validate (i) the AoED as the QoS in decision-making on an event through embedded processing capabilities of sensors and (ii) the energy cost of the network.

B. Methodology

In our implementation, the wireless sensor nodes adopted are called 'SHM mote', as shown in Fig. D. This is a multi-metric and specialized SHM mote with on-board signal processing and embedded decision-making specifically planned for general SHM applications is designed. Each SHM mote is integrated with three main hardware components: a sensor board, an Intel Imote2, and a radio-triggered wakeup with synchronization module. The Imote2 is with an AM radio

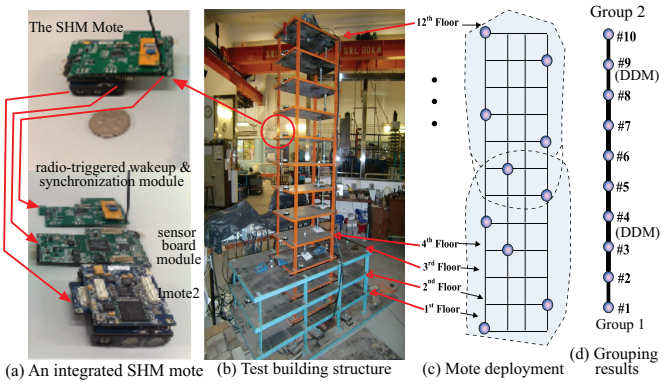

Fig. D. (a) An integrated Imote2 (SHM mote) used in our experiments; (b) Twelve-story test building structure and the placement of 10 SHM motes on it; (c) sensor grouping; (d) DDM selection.

receiver for synchronized sensing and a RF amplifier. It is built around the low-power PXA271 processor and 802.15.4-compliant radio (Chipcon CC2420) with a built-in 2.4GHz antenna. It has 256 KB of embedded SRAM and can address 32 MB of on-board SDRAM,providing plentiful space for data-intensive SHM. For a structure with 'no event of damage', each mote keeps 20 to 22 bytes of data, but removes other data after each T_d. The model-based localized decision-making algorithm is successfully embedded on the Imore2. The fact that the proposed decision-making in this report does not take much computation, the PXA271 speed is scaled down, which allows for an increased performance and energy cost reduction.

In our implementation, we get a very useful from a ISHMP toolsuite (http://shm.cs.uiuc.edu/), which provides subsystems for sensor data acquisition and reliable data transmission. The SHM motes run modified TinyOS, and are configured to sample the accelerometers in a synchronized manner at a frequency of 560Hz. We modify the radio-related components in TinyOS 2.0 for time-stamping the packet close to the transmitter. This makes the time-stamping as close as possible to the first byte transmission, and the first byte reception of the packet. This eliminates the transmission and reception time delays for the data packet. When a mote receives an ACK (acknowledgment) that the data packet is received by an upstream mote (i.e., DDM), then data is removed from the buffer, except for the last set of data that remains in the buffer before monitoring period is over. To carry out our localized algorithms, the network architecture is homogeneous; however, the functions vary when their role changes as an LDM, DDM or BS.

The general sensor board has digital accelerometer with analog input applications. The Imote2's 3D accelerometer has a resolution of 12-bit, or equivalent 0.97 mg with 3-axis of measurement and $\pm 2g$ of amplitude. The AD converter has also digital filters with user-defined cutoff frequencies. Specifications for the accelerometer explain that once the decimation factor is defined, the sampling frequency and corresponding cutoff frequency will have a value within $\pm 10\%$ of the value given.

C. System Deployment

A twelve-story shear frame structure is employed, as shown in Fig. D(b). The lateral stiffness of each floor originates from the four vertical steel columns, 3.81cm by 3.81cm. The twelve-floor structure is shared into two substructures with each having at least four floors. 10 SHM motes are deployed,as shown in Fig. D(b). We consider two substructures of the test structure, where each substructure includes at least 4 floors. In the middle of each substructure considered as the reference sensor point. In the experiment, R_{min} and R_{max} is are set according to d of each substructure and to the distance between the reference sensor point and the BS's location, respectively. It is not difficult to adjust since Imote2 supports discrete levels of range (R_{min} to R_{max}). We choose this so that at a maximum power level, all nodes can talk directly to each other with in a substructure (group-wise).

Under this transmission power level, the topology of the network along with the simplified structure is illustrated in Fig. D(c). Under R_{min}, the topology of the network along with the physical structural elements is illustrated in Fig. D(d). All of the SHM motes organized them into groups according to the reference sensor point location on the structure. All of the SHM motes are programmed with the code for the embedded algorithm and recording group information according to the SOSO algorithm. At the start of the procedure, the BS node propagates a configuration packet to all other nodes in the network.

An extra additional mote is used as the BS node (the remote SHM mote) that is connected to the PC via USB for the control purpose, while this BS node can be removed in future implementation. Java application and MATLAB scripts running on the PC, which are used to set initial command and parameters and functions on SHM motes. For debugging purposes, our system can also retrieve the last set of raw sensor readings from individual mote, which is left after T finishes. To produce a sizable vibration response from the test structure, we collect the original data by vertically exciting the test structure using a magnetic shaker for continuous and modal hammer for instant excitations, which yield reasonably higher structural system responses compared to a real structure. Moreover, in order to obtain realistic results, enough excitation is injected into system to get measurements with a good signal-to-noise ratio. In fact, this excitation level yields reasonably high structural responses that are measured compared to a real high-rise structure or bridge.

APPENDIX F
FURTHER SYSTEM DEPLOYMENT ON AN OUTDOOR STRUCTURE

A. Objectives

As further proof-of-concept experiments on an outdoor structure, we have conducted experiments on the LSK building located at our university campus, as shown in Fig. E.1 (the actual names are anonymous). The objective of this deployment is to validate the feasibility of the decision-making and SOSO algorithms of MODEM. We particularly intend to observe how MODEM performs in practice.

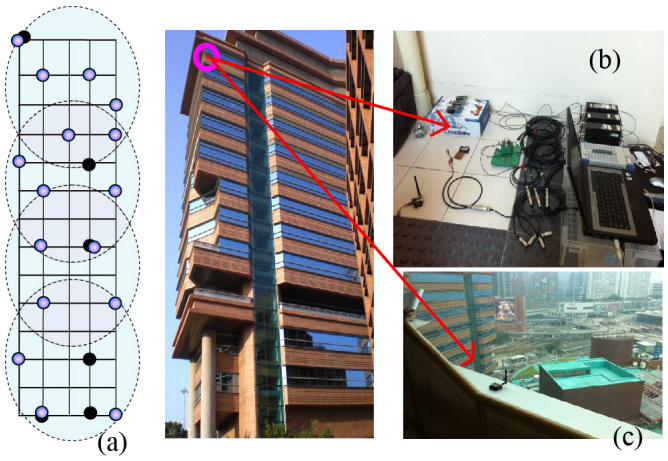

Fig. E.1. Sensor deployment on LSK building: (a) an example of FEM model where 22 SHM mote are placed; (b) BS mote location; (c) the placement of a sensor.

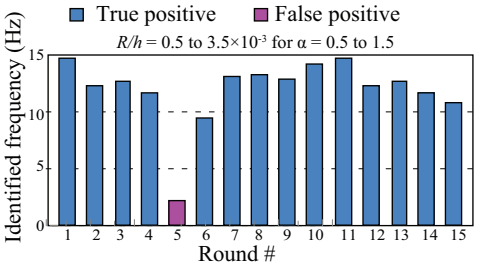

Fig. E.2. Experimental WSN performance: decision-making by a sensor (the 5th) in its different rounds of monitoring.

B. Methodology

We use system configurations similar to the configurations used in our experiments on the lab-based structure. In this deployment, we have selected 22 locations for 22 SHM motes that seem to capture the overall vibration frequency and mode shapes of the structure. We deploy the system three times in three different days and estimate average results.

Similar to the damage event information injection into data traces of sensors during the simulations, or the physical damage event injection into the lab-based structure, we do not have access to inject physical damage event in the LSK tower building. It is not feasible to get real damage event in a healthy structure. Instead, we have used a magmatic shaker to excite the structure around some sensor locations, namely the sensor located at the 5th floor and the 9th floor. We think the excitation level captured by those sensors should be higher than other sensors, which can be considered a lower strength of event detection. Recall that similar case may occur during the incidents of earthquake, hurricane, heavy wind, and so on. As a result, the system should be able to detect such an event that has minimum changes in the dynamic process of the structure.

C. Experimental Results

We first have a look at the decision-making by the 5th LDM sensor in different rounds of monitoring in Fig. E.2. We can see that 5th the sensor makes a false positive decision at round

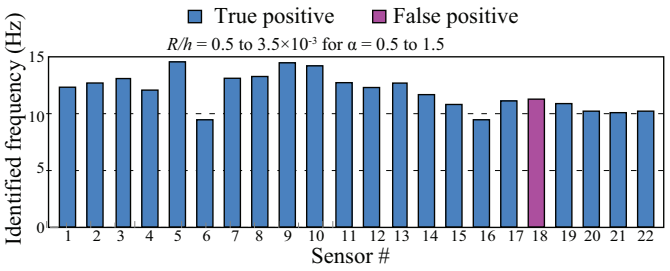

Fig. E.3. Experimental WSN performance: decision-making by all of the sensors in the WSN in a round of monitoring.

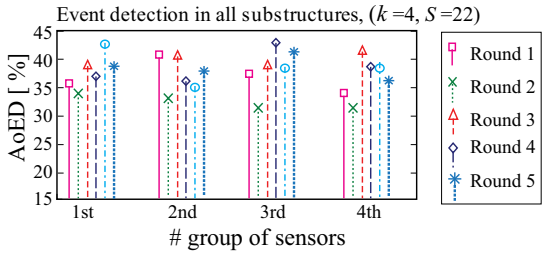

Fig. E.4. Experimental performance: the AoED obtained from five rounds of monitoring operation.

5. However, the final decision came from the the first group of sensors are true positive. Such a single false positive decision cannot deviate the systems from making true positive decision at the DDM (group-wise). If it is false decision (caused by faults, interferences, other related reasons), the false decision can be detected at the LDM when fusing the decisions from all the sensors. Even, in the immediate round of monitoring, such a false positive decision is not seen further at 5th sensor and its neighboring sensors.

Fig. E.3 presents the decisions of all of the sensors of four groups. Fig. E.4 depicts the experimental AoED from five rounds of monitoring operation. It shows that MODEM can provide a sufficient level of AoED under the forced vibration excitations. This implies that MODEM has the ability of those event detection, such earthquake, hurricane, heavy wind, load, etc. The maximum AoED is 38% obtained by some sensors in some group in case of such a low level event. Note that if there occurs a real event of damage in such the structure, the AoED will be increased, similar to the AoED achieved in the lab-based structure.

REFERENCES

[1] B. Li, D. Wang, F. Wang, and Y. Q. Ni, "High quality sensor placement for SHM systems: Refocusing on application demands," in *Proc. of IEEE INFOCOM*, 2010, pp. 1–9.

[2] Y. Ni, Y. Xia, W. Liao, and J. Ko, "Technology innovation in developing the structural health monitoring system for Guangzhou New TV Tower," *Struct. Cont. and Health Monit.*, vol. 16, no. 1, pp. 73–98, 2009.

[3] Z. Xing and A. Mita, "A substructure approach to local damage detection of shear structure," *Structural Control and Health Monitoring*, vol. 19, no. 2, pp. 309–318, 2012.

[4] M. Z. A. Bhuiyan, G. Wang, J. Cao, and J. Wu, "Sensor placement with multiple objectives for structural health monitoring," *ACM Transactions on Sensor Networks*, vol. 10, no. 4, pp. 1–45, 2014.

[5] Y. Chen and A. Terzis, "On the implications of the log-normal path loss model: An efficient method to deploy and move sensor motes," in *Proc. of ACM SenSys*, 2011, pp. 26–39.

[6] T. S. Rappaport, *Wireless Communications: Principles & Practices*. Prentice Hall, 1996.

[7] M. Z. A. Bhuiyan, G. Wang, J. Cao, and J. Wu, "Deploying wireless sensor networks with fault tolerance for structural health monitoring," *IEEE Transactions on Computers*, vol. 64, no. 2, pp. 382–395, 2015.

[8] X. Liu, J. Cao, S. Lai, C. Yang, H. Wu, and Y. Xu, "Energy efficient clustering for WSN-based structural health monitoring," in *Proc. of IEEE INFOCOM*, 2011, pp. 2768 – 2776.

[9] TinyOS documentation. [Online]. Available: http://docs.tinyos.net/tinywiki/index.php/T2_on_Imote2